

## Friction of Gels. 4. Friction on Charged Gels

Jian Ping Gong, Go Kagata, and Yoshihito Osada\*

Graduate School of Science, Hokkaido University, Sapporo 060-0810, Japan

Received: January 22, 1999; In Final Form: April 26, 1999

The friction between two chemically cross-linked polyelectrolyte gels carrying the same sign of charges has been investigated in pure water as well as in salt solutions using a rheometer. It is found that the friction was largely dependent on the charge densities of the gel surface and the ionic strength of the aqueous solution. The chemical structures of the polyelectrolyte gels also play an important role. The friction is described in terms of the hydrodynamic lubrication of the solvent layer between the two gel surfaces, which is formed due to the electrostatic repulsion of the two gel surfaces. The thickness of the solvent layer has been estimated using the Poisson–Boltzmann equation supposing that the ionic osmotic pressure is balanced by the normal pressure applied on the gel. The friction values have been calculated by considering the shear flow of solvent in gel region using the Debye–Binkman equation. For strongly charged polyelectrolyte gels swollen in pure water, the theoretical analysis shows that the friction coefficient almost has no dependence on the water content of the gel, which well agrees with the experimental observations.

### I. Introduction

In the preceding papers,<sup>1,2</sup> we have reported that hydrogels show very low friction forces when slid against themselves or against solid substrates. The friction coefficients of the gels is comparable or even smaller than those of animal cartilage.<sup>3–7</sup> The low gel friction coefficients cannot be explained in terms of a hydrodynamic lubrication mechanism since they are sustained even at a Sommerfeld number as small as  $10^{-11}$ , where the hydrodynamic lubrication can usually never be realized for friction between two solids.<sup>2,8,9</sup>

To describe the frictional behavior of a gel sliding on a solid surface, we have proposed a model from the viewpoint of polymer–solid surface repulsion and adsorption in a previous paper.<sup>10</sup> When a polymer solution is placed in contact with a solid wall, the polymer chain would be either repelled from or adsorbed on the solid wall, depending on the strength of the interaction between them in comparison with the solvent. The behavior of a cross-linked gel surface is similar to that of a polymer solution when in contact with a solid wall. The polymer network on the surface of the gel will be repelled from the surface if it is repulsive, or it will be adsorbed to the solid surface if it is attractive. In the former case, the viscous flow of solvent between the solid surface and the polymer network will make a dominant contribution to the frictional force. In the latter case, however, the adsorbing chain will be stretched when the solid surface makes a motion relative to the gel. The elastic force increases with the deformation and eventually detaches the adsorbing polymer network from the substrate, which in turn appears as the frictional force.

Surface adhesion between glass particles and gels measured by atomic force microscopy showed a good correlation with the friction of gels on a glass surface, which supports the polymer repulsion–adsorption model proposed by the authors.<sup>2</sup>

According to the above consideration, low friction can be realized when two repulsive surfaces slide against each other, since under this condition, it is favorable for low molecular weight solvent to exist between the interface gap and to serve

as a lubricating layer. Therefore, the stronger the repulsion between the two surfaces and the more solvent that exists at the interface, the lower the friction. To obtain a thicker solvent layer, which leads to lower friction, surfaces with strong electrostatic repulsion are expected to be effective.

This paper consists of two parts. In the first part, the effect of electrostatic repulsion on the friction has been investigated experimentally in the following ways: (1) changing the charge density of polyelectrolyte gels by (a) modulating the polymer network density of the gel and (b) copolymerizing polyelectrolyte with neutral polymer and (2) changing the ionic strength of solvent. In the second part, theoretical modeling has been proposed using the Poisson–Boltzmann equation to evaluate the solvent layer thickness and the Debye–Binkman equation to describe the solvent flow in the gel region. The theoretical values are compared with the experimental observations, and the essential feature of the mechanism proposed is confirmed.

### II. Experimental Observations

**II-1. Experiments. Materials.** 2-Acrylamido-2-methylpropanesulfonic acid (AMPS) (Tokyo Kasei Co., Ltd) was used as received. Its sodium salt (NaAMPS) was obtained by neutralization of AMPS with sodium hydroxide (Junsei Chemical Co., Ltd.). *N,N'*-Methylenebisacrylamide (MBAA) (Tokyo Kasei Co., Ltd) used as a cross-linking agent was recrystallized from ethanol. Potassium persulfate (Tokyo Kasei Co., Ltd), which was used as a radical initiator, was recrystallized from water. Sodium *p*-styrenesulfonate (NaSS) (Wako Junyaku Co., Ltd), quaternized *N*-[3-(dimethylamino)propyl]acrylamide (DMA-PAA-Q) (Kohjin Co., Ltd.), and acrylamido (AAm) (Tokyo Kasei Co., Ltd) were used as received.

**Gel Preparation.** Poly(2-acrylamido-2-methylpropanesulfonic acid) (PAMPS) and its sodium salt (PNaAMPS) gels were prepared by radical polymerization of a 1.0 mol/L aqueous solution of AMPS (or NaAMPS) monomer in the presence of a calculated amount of MBAA and 0.001 mol/L potassium persulfate. The polymerization was carried out at 60 °C for 12

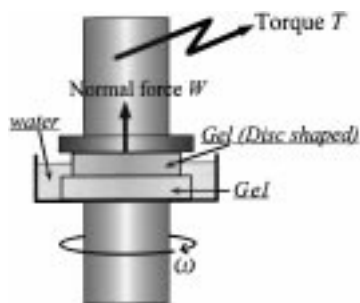


**Figure 1.** Schematic illustration of the rheometer used to measure the gel friction.

h under a nitrogen atmosphere. PAMPS gels with different water content or degree of swelling were prepared by changing the amount of cross-linking agent MBAA from 6 to 20 mol % against the AMPS monomer.

Poly(sodium *p*-styrenesulfonate) (PNaSS) gel and poly-(quaternized *N*-[3-(dimethylamino)propyl]acrylamide) (PDMA-PAA-Q) gel with 12 and 8 mol % of MBAA, respectively, were prepared with the same method as that of PAMPS gel.

Copolymer gels of AAm and NaAMPS (poly(AAm-co-NaAMPS)) with different compositions were prepared by radical polymerization of NaAMPS with AAm in water, by varying the mole fraction of AAm, in the presence of 8 mol % MBAA.

Copolymer gels of AAm and DMAPAA-Q (poly(AAm-co-DMAPAA-Q)) with different compositions were prepared in the same way as that of poly(AAm-co-NaAMPS) with 12 mol % MBAA. The detailed procedure of the polymerization was described elsewhere.<sup>11–13</sup>

Gel samples were prepared between two parallel glass plates separated by a spacer of 1 mm thick to give sheet-shaped gels. After polymerization, the glass plates were removed and sample gels were immersed in a large amount of water for 1 week to equilibrate and wash away the residual chemicals.

**Measurements.** Gel friction measurements were made at the equilibrium swelling state in pure water or in NaCl salt solutions. The amount of water contained in gels, is characterized by the degree of swelling,  $q$ , which is defined as  $q = (\text{swollen sample volume})/(\text{dry sample volume})$ . We approximately calculated  $q$  as the weight ratio of swollen gel to dry gel. Dry gel was obtained by evacuating until it reached a constant weight. The weight percentage of water in a gel ( $w - \text{wt } \%$ ) can be obtained using the relation of  $w - \text{wt } \% = (q - 1)/q \times 100\%$ .

The friction force of the gels was measured in water or in NaCl aqueous solution at 25 °C using a commercialized rheometer (3ARES-17A, Rheometric Scientific F. E. Ltd.) which is shown in Figure 1. The as-prepared surface of the gel was used for the measurements. All samples except PAMPS gel were cut into a disk shape of 15 mm in diameter and then were glued on the upper surface of coaxial disk-shaped platens. Due to the difficulty in gluing a PAMPS gel to the metal platen, a square-shaped PAMPS gel with a side length of 13 mm was crapped on the upper surface of the platen. Another piece of gel a little larger than that of the upper surface gel was fixed at the lower platen. The interface was immersed in water or NaCl solutions. The torque and the normal force were detected when the lower platen rotates with an angular velocity  $\omega$ , at a strain-constant mode. Since the rotation velocity changes with the distance from the center of the axis, the obtained torque,  $T$ , is a total value over the velocity range from 0 to  $\omega R$ , where  $R$  is the radius of the gel. From our previous work,<sup>1,2</sup> the gel friction force is linearly proportional to the apparent contact area under a

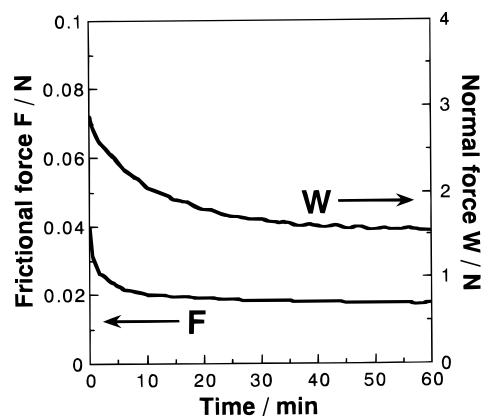


**Figure 2.** Time profiles of friction force and normal force when two pieces of PAMPS gels undergo relative angular rotation in water. Sample radius  $R = 7.5$  mm; angular velocity  $\omega = 0.01$  rad/s; initial normal force  $W = 3$  N.

constant normal pressure. Thus, the frictional force can be expressed in terms of force per unit area. Supposing that the friction is linearly proportional to the velocity, so the friction per unit area at a distance  $r$  from the axis is

$$f = A\omega r \quad (1)$$

where  $A$  is a value not dependent on  $r$ . The total force is

$$F = \int_0^R 2\pi r f dr = (2/3)\pi A\omega R^3 \quad (2)$$

and the total torque is

$$T = \int_0^R 2\pi r f r dr = (\pi/2)A\omega R^4 \quad (3)$$

Therefore, the total friction is determined by

$$F = 4T/3R \quad (4)$$

This relation can be extended to the more general case when  $f \sim (\omega r)^\alpha$ , where  $\alpha$  is a constant,

$$F = \frac{(\alpha + 3)T}{(\alpha + 2)R} \quad (5)$$

In the present study, the friction values were obtained by dividing the torque  $T$  by  $3R/4$ . In the case of PAMPS gel,  $1/\sqrt{2}$  of the side length of the square was used as  $R$ .

The force due to the viscous friction of water exerted on the cylindrical wall of the platens is confirmed to be extremely small in comparison with the friction force and does not bring any inaccuracy to the experimental data. Using a rheometer to measure the friction has several advantages over the tribometer that was used in our previous work.<sup>1,2</sup> One advantage is the possibility of measuring the gel–gel friction with small gel samples. The other is its high sensitivity in detecting the friction force that is encountered in measuring the extremely low friction of gels. One disadvantage of the rheometer is that it can only work in strain constant mode, which leads to a changing normal force due to relaxation.

**II-2. Results and Discussion.** Figure 2 shows the time profiles of the friction force as well as the normal force when two PAMPS gels undergo relative rotation in pure water. The friction force decreases rapidly with time at the beginning of the measurement and becomes constant after 30 min. Since the rheometer runs in a strain-constant mode, the normal force,  $W$ ,

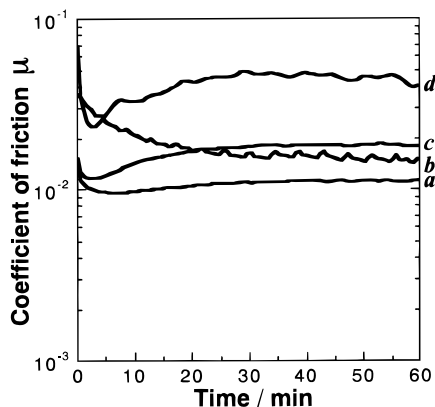


**Figure 3.** Time profiles of coefficients of friction when two pieces of polyelectrolyte gels of the same kind undergo angular rotation in water. Sample radius  $R = 7.5$  mm; angular velocity  $\omega = 0.01$  rad/s: (a) PAMPS gel; (b) PNaAMPS gel; (c) PNaSS gel; (d) PDMAA-Q gel. Initial normal force  $W = 3N$ .

decreases with the time and reaches a constant value after 30 min. Thus, the change in the friction force,  $F$ , well corresponds with that of the normal force relaxation.

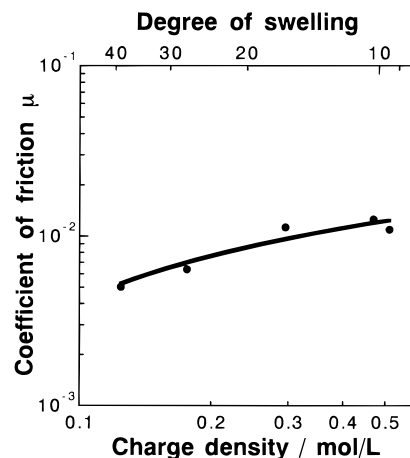
The coefficient of friction,  $\mu$ , that is obtained by the relation of  $\mu = F/W$  from Figure 2 is shown in Figure 3. The value of  $\mu$  shows a minimum at the initial stage of measurement and then becomes almost constant with time after 20 min.

Figure 3 also shows the time profiles of the coefficient of friction for various kinds of polyelectrolyte gels rotating in water. Polyanion gel of PNaSS and the polycation gel of PDMAA-Q also showed a minimum in the friction coefficient at the initial time, which is similar with that of PAMPS gel. However, PNaAMPS, which has the same chemical structure of its polymer network as PAMPS gel but with  $Na^+$  as counterions instead of  $H^+$ , showed a monotonic decrease in the coefficient of friction with time at the initial 30 min of measurement and then becomes constant. All these gels show small and stable values of friction after 30–40 min. The three polyanion gels showed approximately the same friction coefficients in the range of  $(1-2) \times 10^{-2}$  at the stable state. However, the friction of the polycation gel of PDMAA-Q is about 4 times higher than that of polyanion gels.

However, when a pair of polyelectrolyte gels with opposite charges, for example, PAMPS gel with PDMAA-Q gel, were slid over each other, the adhesion between the two gel surface was so high that the gels were broken in the measurement. This strong adhesion should apparently be attributed to the electrostatic attraction between polyanions and polycations of the gels.

The above experimental results demonstrate that the friction is largely dependent on the electrostatic interaction between the two gel surfaces. The low friction between two polyelectrolyte gels carrying the same charge should be attributed to the surface electrostatic repulsion of charges fixed on the polymer network.

The different values of friction for various gels as shown in Figure 3 should be associated with their charge density and water content. Thus, we further investigate the effect of charges and the degree of swelling on the friction. The relaxation behaviors in friction at the initial stage of measurement are complicated. Thus, we only concentrate on the friction behavior of gels at a stable state. Figure 4 shows the network charge density dependence of the friction for two pieces of PAMPS gels undergoing relative rotation. All the data were taken after the coefficient of friction became constant. The modulation of charge density of the gel has been made by varying the amount



**Figure 4.** Dependencies of charge density and degree of swelling on friction coefficient of two PAMPS gels in water. Sample radius  $R = 7.5$  mm; angular velocity  $\omega = 0.05$  rad/s; initial normal force  $W = 3N$ .

of cross-linking agent in the process of gel synthesis, which gives rise to gels of different swelling ability. Since the polyelectrolyte gels used in this work fully dissociate in water, carrying one charge at each monomer unit, the charge density,  $c$  (in units of mol/L), equals the polymer network concentration. Therefore,  $c = 1000/qM_w$ , where  $M_w$  is the formula molecular weight of the monomer. As shown in Figure 4, the friction increases modestly with the increase in charge density. That is, the frictional force does not sensitively change with the degree of swelling. Two opposite effects on the frictional force can be considered by examining the increase in charge density: One is the enhanced repulsion between the two gel surfaces, which favors the formation of a thicker solvent layer between the surfaces and decreases the viscous friction. The other is the increased network density, which increases the hydrodynamic resistance of the water in the polymer network and leads to an increase in the frictional force of the gel. A higher water content would lead to a small friction force since the fraction of polymer network which is nonflow decreases with the increase in the water content. Therefore, a higher charge density would bring a thicker liquid layer, which leads to a lower friction but gives rise to an increase of nonflow network density, which increases the friction. These two opposite effects on the friction explain why the friction is not sensitive to the network charge density.

An addition of any neutral salt into water can decrease the electrostatic repulsion and favors the approach or the contact of the two repulsive gel surfaces. Thus, the polyelectrolyte gels were immersed in NaCl solutions of various concentrations. After establishing the equilibrium in salt solution, the gels were cut into the same size as that without salt and the friction was measured. Figure 5 shows the results of frictions of PNaAMPS gel, PNaSS gel, and PDMAA-Q gel measured in NaCl solutions of various concentrations. For all three kinds of polyelectrolyte gels, the friction coefficients are almost the same as those in water if the salt concentration is less than  $10^{-2}$  M. However, when NaCl concentration increases further, the friction force increases rapidly and at 1 M NaCl, it increases about 1 order (PNaSS, PDMAA-Q) or 2 orders (PNaAMPS) of magnitude. Here, it should be noted that the degree of swelling of the gel decreases with the increase in salt concentration, as shown in Figure 5, due to the screening of the electrostatic repulsion between charged groups on the polymer chain. Incorporating the volume change of the gel, the charge density in the gel was calculated and the frictional coefficient is plotted

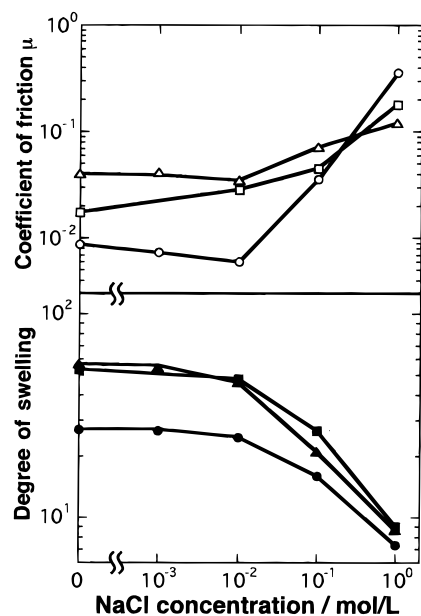


**Figure 5.** Friction coefficients (open symbols) and the degrees of swelling (solid symbols) of polyelectrolyte gels in NaCl solutions: (○,●) PNaAMPS gel; (□,■) PNaSS gel; (△,▲) PDMAPAA-Q gel. Sample radius  $R = 7.5$  mm; angular velocity  $\omega = 0.01$  rad/s; initial normal force  $W = 3N$ .

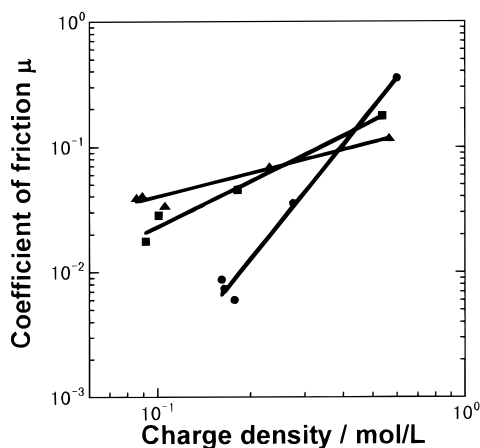


**Figure 6.** Relations between the friction coefficients and the gel charge densities obtained from Figure 5: (●) PNaAMPS gel; (■) PNaSS gel; (▲) PDMAPAA-Q gel.

as a function of the charge density. The results are shown in Figure 6. Contrary to the results in Figure 4, the coefficient of friction increases with the increase in charge density of the polymer network when the ionic strength increases. This experimental result demonstrates that the electrostatic repulsion is effectively screened by the presence of salt, and this allows the polymer chains on the two gel surfaces to approach each other near enough that short distance attraction forces between the polymer networks come into action. The different slopes in Figure 6 for different types of gels might be associated with the difference in the physicochemical nature of the networks.

The effect of charge density was also studied by sliding copolymer gels containing different numbers of ionic monomers on homopolymer gels. Figure 7 shows the friction force when poly(AAm-co-NaAMPS) gels with various composition were allowed to slide on a PNaAMPS gel. The friction between two homopolyelectrolyte gels of PNaAMPS showed the lowest values. With the increase of AAm composition, i.e., decrease of negative charge density, the friction increases and PAAM

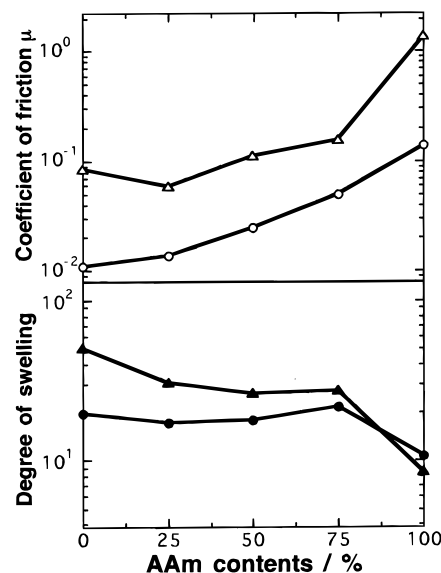


**Figure 7.** Dependencies of the friction coefficient (open symbols) and the degree of swelling (solid symbols) on the copolymer composition. The frictions are the values between poly(AAm-co-NaAMPS) gel and PNaAMPS gel (○,●) or poly(AAm-co-DMA-PAA-Q) gel and PDMA-PAA-Q gel (△,▲) in water. Sample radius  $R = 7.5$  mm; angular velocity  $\omega = 0.01$  rad/s; initial normal force  $W = 3N$ .

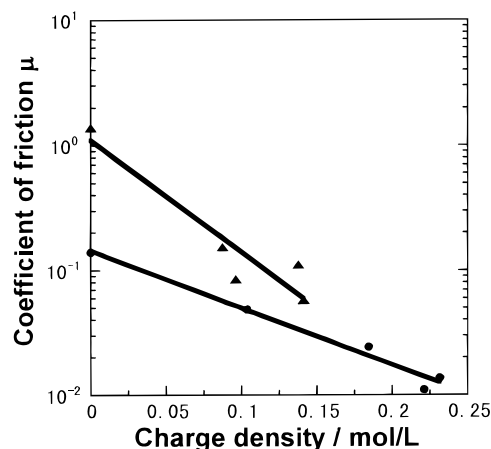


**Figure 8.** Relations between the friction coefficient and the gel charge concentration calculated from Figure 7: (●) poly(AAm-co-NaAMPS) gels; (▲) poly(AAm-co-DMA-PAA-Q) gels.

homopolymer gel showed the highest friction. Similar results were obtained if the poly(AAm-co-DMA-PAA-Q) gels were allowed to slide on the PDMAPAA-Q gel. Taking into account the change in the swelling ratio brought on by changing the copolymer composition, the charge density of the gel was calculated and the relation between the friction coefficient and the charge density of the copolymer gels is plotted as shown in Figure 8. The figure clearly shows that the coefficient of friction decreases with the increase in the charge density. So far, we cannot explain why the poly(AAm-co-DMA-PAA-Q) gel on PDMAPAA-Q gel shows a higher friction than the poly(AAm-co-NaAMPS) gel on PNaAMPS gel. It should be related to the stronger interaction between AAm and DMA-PAA-Q.

From the above results, we could demonstrate that the friction of gels is largely dependent on the charge density of the gels. By varying the charge density of the gel or the ionic strength of the solvent, the friction coefficient of the gel can be varied by about two orders of the magnitude in the examined experimental range.



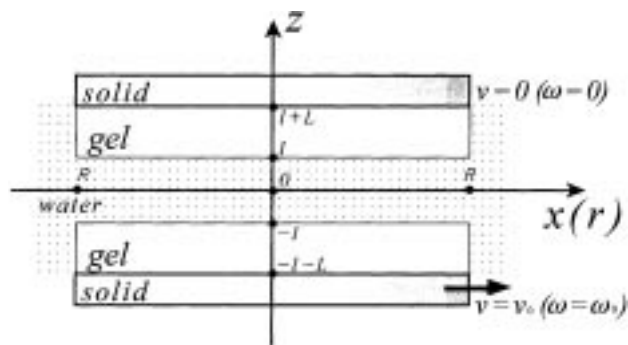


**Figure 9.** The geometry of two polyelectrolyte gel surfaces of the same kind approaching each other in water. Due to the electrostatic repulsion, a water layer  $2l$  in thickness is formed under a normal pressure  $P$ . One of the gels is doing translation (or rotational) motion in a velocity of  $v_0$  (or  $\omega$ ).

### III. Theoretical Analysis

**III-1. Solvent Layer Thickness.** According to the repulsion–adsorption model, the low friction between two polyelectrolyte gels carrying the same charge is a hydrodynamic mechanism, in which the strong electrostatic repulsion plays an important role in forming a solvent layer between the two gel surfaces. Here we estimate the thickness of the solvent layer under a certain load. When the load is not very high, the electrostatic repulsion prevails and the van der Waals interaction between the two surfaces can be neglected. Supposing that the polyions are homogeneously distributed in the bulk gel as well as on the gel surface, then we have an average surface charge density. For a homopolymer gel carrying one charge at each monomer unit, the number surface charge density,  $\sigma$  (in units of  $\text{m}^{-2}$ ), is

$$\sigma = (1000cN_A)^{2/3} = \left(\frac{10^6 N_A}{qM_w}\right)^{2/3} \quad (6)$$

Here,  $c$  is the bulk charge density of the gel or the monomeric concentration (in mol/L) and  $N_A$  is Avogadro's number.

We denote the solvent layer thickness between two gel surfaces as  $2l$  and the gel sample thickness as  $L$ , and we chose the origin of the coordinate system at the middle point between two gel surfaces with the  $x$ -axis parallel to and the  $z$ -axis vertical to the gel surfaces (Figure 9). Here,  $L \gg l$ . Thus, the electrical potential distribution between the two gel surfaces,  $\psi(x)$ , given by Poisson equation is expressed as

$$\nabla\psi(z) = -\rho(z)/\epsilon \quad -l < z < l \quad (7)$$

where  $\epsilon$  is the dielectric constant of water and  $\rho(z)$  is the counterion density at position  $z$ , which is given by the Boltzmann distribution. For positively charged counterions which corresponds to polyanion gels,

$$\rho(z) = en_0 \exp[-e\psi(z)/kT] \quad (8)$$

here,  $n_0$  is the density of counterions at a position where  $\psi = 0$ ,  $e$  is the charge of an elementary electron,  $k$  is the Boltzmann constant, and  $T$  is the absolute temperature. For the simplicity, we only consider the case of monovalent ions. Combining eqs 7 and 8, we have

$$\frac{d^2\psi}{dz^2} = -\frac{en_0}{\epsilon} \exp(-e\psi/kT) \quad (9)$$

On the gel surface,

$$\left(\frac{d\psi}{dz}\right)_{z=\pm l} = \mp \frac{e\sigma}{\epsilon} \quad (10)$$

On the symmetric plane,

$$\left(\frac{d\psi}{dz}\right)_{z=0} = 0 \quad (11)$$

From the electrical neutrality,

$$\sigma = n_0 \int_0^l \exp(-e\psi/kT) dz \quad (12)$$

Equation 9 can be solved analytically. By choosing  $\psi_{z=0} = 0$ , we have

$$e\psi/kT = 2 \ln \cos(\sqrt{n_0 r_0/2} z) \quad (13)$$

where  $n_0$  is a function of the surface number charge density given by

$$\sigma = \sqrt{2n_0 r_0} \tan(l\sqrt{n_0 r_0/2}) \quad (14)$$

here  $r_0 = e^2/\epsilon kT$  is a constant with a dimension of length. The repulsive osmotic pressure  $\Pi$ , between two approaching charged surfaces is determined by the microion charge density at the symmetry plane of  $z = 0$ , where the electrostatic attraction on the microions is zero since  $(d\psi/dz)_{z=0} = 0$ <sup>14</sup> so we have

$$\Pi = n_0 kT \quad (15)$$

In the equilibrium state, this osmotic pressure is counterbalanced by the applied pressure  $P$ , that is,  $P = \Pi$ . Thus, the solvent layer thickness under a normal pressure  $P$  is obtained by combining eqs 14 and 15 and the condition  $P = \Pi$

$$2l = 2\sqrt{kT/Pr_0} \arctan(\sigma\sqrt{kTr_0/2P}) \quad (16)$$

When  $\sigma$  is very small and  $P$  is high so that  $\sigma\sqrt{kTr_0/2P} \ll 1$  is satisfied,  $\arctan(\sigma\sqrt{kTr_0/2P}) \approx \sigma\sqrt{kTr_0/2P}$ . Accordingly,  $2l \propto P^{-1}$ . This inverse relation between the solvent layer thickness and the pressure agrees with eq 5 in ref 10 derived for the repulsive case from the scaling rules. When  $\sigma$  is very large and  $P$  is not too high so that  $\sigma\sqrt{kTr_0/2P} \gg 1$ ,  $\arctan(\sigma\sqrt{kTr_0/2P}) \approx \pi/2$ . Accordingly,  $2l \propto P^{-1/2}$ . This indicates that highly charged surfaces are able to sustain more pressure.

Figure 10 shows the theoretically calculated relations between the solvent layer thickness and the normal pressure  $P$  at various degrees of swelling of the gel. At a high surface charge density, which corresponds to a low degree of swelling, the repulsion distance  $2l$  is not sensitive to the pressure when the pressure is not very high. Notice that the experimental investigation in Figure 4 was performed at  $q = 10\text{--}30$  and  $P \approx 10^4$  Pa. Under these conditions, the solvent layer thickness  $2l$  is not sensitive to the gel surface charge density and it has a value of 30 nm.

When simple salt is added to the system, the Poisson equation cannot be analytically solved. In addition, for high salt concentration, the electrostatic repulsion is extensively screened and the polymer chains can approach each other. Therefore, the van der Waals attraction force should be taken into consideration, and the friction mechanism would change from hydrodynamics to polymer chain detachment. We leave further discussion on this case for future works.

**III-2. Shear Flow of Solvent.** When the two gel surfaces inter-mediated by a water layer of thickness  $2l$  are allowed to undergo relative motion, the shear flow of the water layer exerts

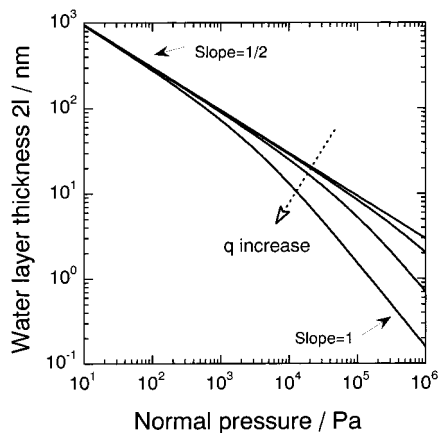


**Figure 10.** Normal pressure dependence of the solvent layer thickness  $2l$  for charged gels with various degree of swelling. Following the direction of the arrow in the figure,  $q = 1, 100, 1000, 10000$ . Parameters used in the calculation:  $\epsilon = 78\epsilon_0$ ,  $T = 300$  K and  $M_w = 229$  ( $M_w$  of NaAMPS).

shear forces on the two gel surfaces and gives rise to the friction. Hence, we need to investigate the velocity profile of the solvent between the two gel surfaces. For simplicity, we first consider the case for two gels undergoing translational motion with the geometry and the coordinates shown in Figure 9. Supposing that the lower surface of the gel slides with a velocity of  $v_0$  in the  $x$ -axis direction while the upper one is fixed. The velocity distribution in the fluid region is determined by

$$\frac{d^2v}{dz^2} = 0 \quad -l \leq z \leq l \quad (17)$$

Since the gel consists of the elastic polymer network and the viscous water, the latter can flow under the shear stress, we cannot simply use a nonslippery boundary condition on the two gel surfaces to solve eq 17. Instead, the velocity profiles in the gel regions should be taken into consideration. The flow of solvent in a polymer network is successfully expressed by the Debye–Brinkman equation, where the effect of polymer network is represented by a distributed body force  $-\eta v/K_{\text{gel}}$ .<sup>15–17</sup> Here  $\eta$  and  $K_{\text{gel}}$  are the viscosity of solvent and the permeability of the gel, respectively. Using the Debye–Brinkman model, the governing equations in the two gel regions are

$$\frac{d^2v}{dz^2} = \frac{v - v_0}{K_{\text{gel}}} \quad -L \leq z \leq -l \quad (18)$$

$$\frac{d^2v}{dz^2} = \frac{v}{K_{\text{gel}}} \quad l \leq z \leq L \quad (19)$$

On the fluid–gel boundaries, we have continuous velocities and continuous shear forces. That is,

$$v_{z=\pm l} \text{ matching} \quad (20)$$

and

$$\left(\frac{dv}{dz}\right)_{z=\pm l} \text{ matching} \quad (21)$$

With these boundary conditions, the solutions of eqs 17–19 are as follows:

$$v = \frac{-v_0 z}{2(l + \sqrt{K_{\text{gel}}})} + \frac{v_0}{2} \quad -l \leq z \leq l (\text{fluid region}) \quad (22)$$

$$v = v_0 - \frac{v_0}{2(1 + l/\sqrt{K_{\text{gel}}})} \exp\left(\frac{l+z}{\sqrt{K_{\text{gel}}}}\right) \quad -L \leq z \leq -l (\text{gel region}) \quad (23)$$

$$v = \frac{v_0}{2(1 + l/\sqrt{K_{\text{gel}}})} \exp\left(\frac{l-z}{\sqrt{K_{\text{gel}}}}\right) \quad l \leq z \leq L (\text{gel region}) \quad (24)$$

Equations 23 and 24 indicates that the velocity exponentially decays from the gel surface with a characteristic decay length of  $\sqrt{K_{\text{gel}}}$ . So the shear stress at the gel surface is

$$f = -\eta \left(\frac{dv}{dz}\right)_{z=\pm l} = \frac{\eta v_0}{2(l + \sqrt{K_{\text{gel}}})} \quad (25)$$

This result indicates that the shear flow can penetrate into the gel with a thickness of  $\sqrt{K_{\text{gel}}}$ , or the equivalent nonslippery boundary of a gel surface is located at a depth of  $\sqrt{K_{\text{gel}}}$  from the gel surface. We should notice that eq 25 is coincident with eq 6 in ref 10 for a repulsive case since the permeable length is equivalent to the end-to-end distance of the subchain strand or the network size of the gel  $\xi$ .

Equation 25 indicates that the friction is inversely proportion to  $l + \sqrt{K_{\text{gel}}}$ .  $\sqrt{K_{\text{gel}}} \cong \xi$  decreases with the increase in the polymer network density. On the other hand, as has been shown,  $l$  increases with the increase of the polymer network density. So the dependence of the parameter  $\xi/l$  on the degree of swelling as well as on the pressure is very important in determining the friction behavior. For strong polyelectrolyte, the chain is fully extended at equilibrium swelling in pure water, so  $\xi = aN$ , where  $a$  is the monomer unit length and  $N$  is the monomer unit number between two cross-linking points.  $N$  can be related with the polymer network concentration of a gel, which corresponds to the overlap concentration  $c^*$  of its polymer solution:<sup>18,19</sup>

$$c^* = N/\xi^3 = a^{-3}N^{-2} \quad (26)$$

So

$$\xi = a\phi^{-1/2} = aq^{1/2} \quad (27)$$

since  $\phi \cong c^*a^3$  and  $q = 1/\phi$ , where  $\phi$  is the polymer network volume fraction. Here, deformation of the polymer network under the pressure  $P$  is neglected. When the pressure is large and comparable with the compressive elastic modulus of the gel,  $E$ ,  $\xi \cong \xi_0/(1 + P/E)^{1/3}$ , where  $\xi_0$  is that without the pressure. For a fully ionized polyelectrolyte gel,<sup>18,19</sup>

$$E \cong kT/a^3q \quad (28)$$

Figure 11 shows the change of  $\xi/l$  on  $q$  for certain pressures. When  $q$  is not too large,  $\xi/l \ll 1$  and the effect of  $\xi$  can be neglected. For very high  $q$ ,  $\xi$  becomes important and should be taken into consideration.

Next, we consider the case of two gel surfaces rotating. For a liquid that exists between two infinitely large coaxial plates rotating, its spatial velocity profile is very complicated.<sup>20,21</sup> Fortunately, for the present case, the Reynolds number of motion,  $\text{Re} \approx \omega_0 l^2/\nu \ll 1$ , so only the angular velocity

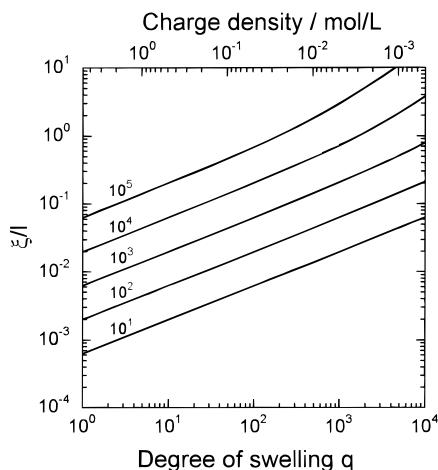


**Figure 11.** Dependence of  $\xi/l$  on the degree of swelling and on the charge density of gels under various normal pressures. The numbers in the figure are normal pressures (in Pa). Parameters used in the calculation:  $\epsilon = 78\epsilon_0$ ,  $T = 300$  K, and  $M_w = 229$  (Mw of NaAMPS),  $a = 0.3$  nm.

component is predominant.<sup>20</sup> Therefore, the angular velocity should take a form similar to the translational velocity of eqs 22–24,

$$\omega = \frac{-\omega_0 x}{2(l + \sqrt{K_{\text{gel}}})} + \frac{\omega_0}{2} \quad -l \leq z \leq l \quad (29)$$

$$\omega = \omega_0 - \frac{\omega_0}{2(1 + l/\sqrt{K_{\text{gel}}})} \exp\left(\frac{l+z}{\sqrt{K_{\text{gel}}}}\right) \quad -L \leq z \leq -l \quad (30)$$

$$\omega = \frac{\omega_0}{2(1 + l/\sqrt{K_{\text{gel}}})} \exp\left(\frac{l-z}{\sqrt{K_{\text{gel}}}}\right) \quad l \leq z \leq L \quad (31)$$

The shear stress on the gel surfaces at a distance  $r$  from the axis is

$$f = -\eta r \left( \frac{d\omega}{dz} \right)_{z=\pm l} = \frac{\eta r \omega_0}{2(l + \sqrt{K_{\text{gel}}})} \quad (32)$$

So the total friction for a disk-shaped gel of radius  $R$  is

$$F = \int_0^R 2\pi r f dr = \frac{\pi \eta \omega_0 R^3}{3(l + \sqrt{K_{\text{gel}}})} \quad (33)$$

From the above equation, we know that the friction per unit area is proportional to the angular velocity and the radius of the gel, since the average velocity increases with the radius. Figure 12 shows the simulation results for the dependence of friction coefficient

$$\mu = \frac{F}{\pi R^2 P} \quad (34)$$

on the water content for two polyelectrolyte gels of the same kind undergoing relative rotation at a certain applied pressure. At a wide range of  $P$ , the friction is not sensitively dependent on the degree of swelling. This is due to the cancellation of the opposite effects of the degree of swelling on the solvent layer thickness and on the gel permeability,  $K_{\text{gel}}$  as discussed previously. Figure 13 shows the normal pressure dependence of friction for gels with various degree of swelling. The friction

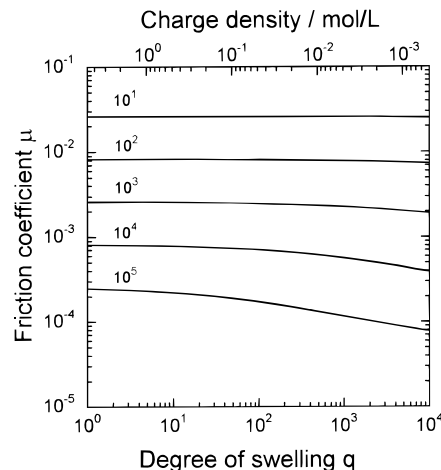


**Figure 12.** Dependencies of the friction coefficients on the degree of swelling and on the charge density for two charged gels undergoing relative rotation. Numbers in the figure are the normal pressure (in Pa). Parameters used in the calculation:  $\omega = 0.05$  rad/s,  $R = 7.5$  mm, and  $\eta = 10^{-3}$  N s/m<sup>2</sup> (bulk water viscosity). Other parameters used are the same as those used in Figure 11.

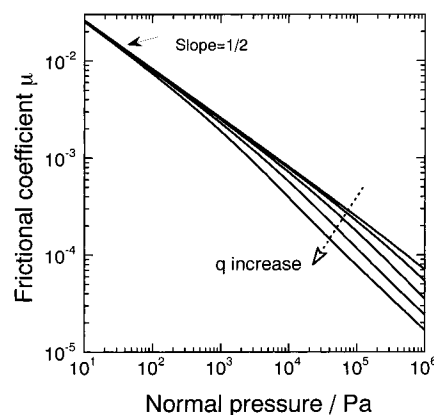


**Figure 13.** Relationship between the normal pressure and the friction coefficient for two charged gels undergoing relative rotation. Following the direction of the arrow in the figure, the degree of swelling of the gel  $q = 1, 10, 100, 1000, 10000$ . Parameters used in the calculation are the same as those used in Figure 12.

coefficient decreases with the increase in the normal pressure and it approximately follows a power law of  $\mu \sim P^{-3/5}$  regardless of the change in the degree of swelling. Figures 12 and 13 well explain why the observed friction in Figure 4 is not sensitively dependent on the degree of swelling.

Under the experimental condition of  $10^4$  Pa, Figure 13 gives out a friction coefficient  $\mu \sim 10^{-3}$ . This simulation value with no free parameter is about 1 order lower than that of experimental observation. This discrepancy may be associated with the presence of so-called “bound water”. As has been well-established, the thermal movement of water molecules located adjacent to the macroions is locally restricted and the <sup>1</sup>H NMR spin–lattice relaxation time<sup>22</sup> is low due to strong attractive interaction with macrocharges located nearby. This suggests that the water molecules located within a certain distance from the macroions hardly move out from the potential energy valley made by the charged network. On the other hand, free water existing far from the ionic “atmosphere” can easily migrate under the out stimuli such as electric field, hydrostatic pressure, or, in the present case, the shear force. From our previous research on the electric field induced contraction of PAMPS gels,<sup>23</sup> which occurs due to the electro-osmotic migration of

water in the gel, about 148 water molecules per sulfonate moiety are bound to the polymer chain strongly and not displaced by electric field. This corresponds to water molecules absorbed around the macroions at a thickness of 3–4 times the radius of the macroions. Our previous experimental research also showed that the electro-osmotic migration velocity of water in the PAMPS gels is only  $1/10$  of that from theoretical estimation, in which the free water viscosity had been used also. Therefore, using the bulk viscosity value of water would largely underestimate the friction force. An effective viscosity of water should be taken into consideration in future work.

Although there is a disagreement in the absolute value of friction force between our theoretical model and the experimental observations, the theoretical prediction qualitatively demonstrates the hydrodynamic nature of the friction between strongly repulsive gel surfaces.

**Acknowledgment.** This research was supported by Grant-in-Aid for the Specially Promoted Research Project “Construction of Biomimetic Moving System Using Polymer Gels” from the Ministry of Education, Science and Culture, Japan.

## References and Notes

- (1) Gong, J. P.; Higa, M.; Iwasaki, Y.; Katsuyama, Y.; Osada, Y. *J. Phys. Chem.* **1997**, *101*, 5487.
- (2) Gong, J. P.; Iwasaki, Y.; Osada, Y.; Kurihara, K.; Hamai, Y. *J. Phys. Chem. B* **1999**, *103*, 6001.
- (3) McCutchen, C. W. *Wear*, **1962**, *5*, 1.
- (4) McCutchen, C. W. *Lubrication of Joints, The Joints and Synovial Fluid*, Academic Press: New York, 1978, *10*, 437.
- (5) Dowson, D.; Unsworth, A.; Wright, V. *J. Mechn. Eng. Sci.* **1970**, *12*, 364.
- (6) Ateshian, G. A.; Wang, H. Q.; Lai, W. M. *J. Tribol.* **1998**, *120*, 241.
- (7) Hodge, W. A.; Fijian, R. S.; Carlson, K. L.; Burgess, R. G.; Harris, W. H.; and Mann, R. W. *Proc. Natl. Acad. Sci. U.S.A.* **1986**, *83*, 2879.
- (8) Adamson, A. W. *Physical Chemistry of Surfaces*; John Wiley & Sons: New York, 1990.
- (9) Persson, B. N. J. *Sliding Friction, Physical Principles and Applications*; Springer: 1998.
- (10) Gong, J. P.; Osada, Y. *J. Chem. Phys.* **1998**, *109*, 8062.
- (11) Narita, T.; Gong, J. P.; Osada, Y. *J. Phys. Chem. B* **1998**, *102*, 4566.
- (12) Gong, J. P.; Kawakami, I.; Sergeyev, V. G.; Osada, Y. *Macromolecules* **1991**, *24*, 5246.
- (13) Kim, B. S.; Ishizawa, M.; Gong, J. P.; Osada, Y. *J. Polym. Sci.: Part A: Polym. Chem.* In press.
- (14) Buschmann, M. D.; Grodzinsky, A. J. *J. Biomech. Eng.* **1995**, *117*, 179.
- (15) Brinkman, H. C. *Physica* **1947**, *13*, 447.
- (16) Wiegell, F. W. *Lecture Notes in Phys.*; Springer: Berlin, 1980; p 121.
- (17) Ethier C. R. and Kamm, R. D. *PCH PhysicoChem. Hydrodyn.* **1989**, *11*, 219.
- (18) Rubinstein, M.; and Colby, R. H. *Phys. Rev. Lett.* **1994**, *73*, 2776.
- (19) Dobrynin, A. V.; Colby, R. H.; and Rubinstein, M. *Macromolecules* **1995**, *28*, 1859.
- (20) Mellor, G. L.; Chapple, P. J.; Stokes, V. K. *J. Fluid Mech.* **1968**, *31*, 95.
- (21) Roberts, S. M.; Shipman, J. S. *J. Fluid Mech.* **1976**, *73*, 53.
- (22) Yasunaga, H.; Ando, I. *Polym. Gels Networks*, **1993**, *1*, 83.
- (23) Gong, J. P.; Nitta, T.; Osada, Y. *J. Phys. Chem.* **1994**, *98*, 9583.